A Study on Applying Slide-Free Label-Free Harmonic Generation Microscopy For Noninvasive Assessment of Melasma Treatments With Histopathological Parameters

Ming-Liang Wei, Yi-Hua Liao, Wei-Hung Weng, Yuan-Ta Shih, Yi-Shuan Sheen, and Chi-Kuang Sun, *Fellow, IEEE*

***Abstract*—Melasma, which is thought to be associated with hyperactivation of melanocytes, is a common hyperpigmentary skin disorder. To treat this skin disorder, dermatologists can benefit from in vivo information of cellular morphometrics to evaluate pathologies of melasma and effectiveness of treatments. To acquire this useful information, we applied the in vivo slide-free label-free harmonic generation microscopy (HGM) to retrieve real-time HGM images and subsequent critical histopathological parameters. These in vivo quantitative parameters included melanin mass density (MMD), melanocyte dendricity score (MDS), melanophage density (MPD), and thickness of dermal papilla zone (DPZ). The statistical results from 33 recruited Asian female melasma patients showed that MMD, MDS, and MPD in melasma lesions were significantly higher than those in the surrounding normal skin; by contrast, the DPZ was lower. After treatment, the MMD, MPD, and DPZ restored toward the normal level; however, we observed no significant change of MDS. Our study indicates that these parameters are able to serve as clinical indices to evaluate the histopathological characteristics of melasma patients and the effectiveness of treatments.**

***Index Terms*—Harmonic generation microscopy (HGM), in vivo melanocyte activity, melanin mass density (MMD), melasma.**

Manuscript received September 30, 2020; revised March 14, 2021; accepted March 24, 2021. Date of publication March 31, 2021; date of current version May 7, 2021. This work was supported in part by MOST of Taiwan under the project of MOST 109-2823-8-002-004, MOST 107-2221-E-002-157-MY3, and in part by grants from NHRI of Taiwan under the project of NHRI-EX105-9936EI. *(Corresponding authors: Chi-Kuang Sun; Yi-Hua Liao.)*

Ming-Liang Wei and Yuan-Ta Shih are with the Molecular Imaging Center, Graduate Institute of Biomedical Electronics and Bioinformatics, National Taiwan University, Taipei 10617, Taiwan (e-mail: b89205102@gmail.com; poundshih@gmail.com).

Yi-Hua Liao and Yi-Shuan Sheen are with the Department of Dermatology, National Taiwan University Hospital, Taipei 10002, Taiwan, and also with the Department of Dermatology, College of Medicine, National Taiwan University, Taipei 10617, Taiwan (e-mail: yihualiao@ntu.edu.tw; sheenyishuan@gmail.com).

Wei-Hung Weng is with the Molecular Imaging Center, Graduate Institute of Biomedical Electronics and Bioinformatics, National Taiwan University, Taipei 10617, Taiwan, and also with the Department of Electrical Engineering and Computer Science, MIT, Cambridge, MA 02139 USA (e-mail: ckbjimmy@mit.edu).

Chi-Kuang Sun is with the Department of Electrical Engineering, Graduate Institute of Photonics and Optoelectronics, Graduate Institute of Biomedical Electronics and Bioinformatics, and Molecular Imaging Center, National Taiwan University, Taipei 10617, Taiwan (e-mail: sun@ntu.edu.tw).

Color versions of one or more figures in this article are available at https://doi.org/10.1109/JSTQE.2021.3069472.

Digital Object Identifier 10.1109/JSTQE.2021.3069472

I. Introduction

MELASMA, caused by hyperpigmentation of melanin and thought to be associated with hyperactivation of melanocytes, is a common hyperpigmentary skin disorder found frequently on both sides of the face. Sivayathorn *et al.* [1], [2] have observed that the prevalence of melasma in some Southeast Asian populations can be up to 40% in females and 20% in males. Histopathologically, melasma is characterized by epidermal hyperpigmentation [3], increased number of melanocytes [3], modification on the extracellular matrix [4], and perivascular lymphohistiocytic infiltrates [5]. Unfortunately, the exact mechanisms of this common skin disorder are not well understood [6].

Despite the unclear mechanisms, melanocytes, especially their activity, are generally considered to be the keystone in the mechanism of melasma. Akabane *et al.* [6] pointed out that melasma was thought to be UV-induced or hormone-induced hyperactivation of melanocytes. According to the past research with a traditional skin biopsy and the followed suitable immunostaining for melanocytes, the number of epidermal melanocytes [7], staining intensity [7], dendricity [8], and even activation status [8] in melasma lesions were significantly higher than those in normal skin. For example, Kang *et al.* [7] stated that 47 of 56 cases (84%) showed an increased number of melanocytes in melasma lesions. These ex vivo histopathological parameters of cellular morphometrics, including the number and dendricity of melanocytes, are considered to be critical parameters to determine the pathogenesis.

Dermatologists usually diagnose melasma patients by examining their skin with the naked eye or a Wood's light, rather than using invasive biopsy. As concluded by Pandya *et al.* [9], Melasma Area and Severity Index (MASI) and mMASI (modified Melasma Area and Severity Index, a clinical index defined and modified from MASI) are the most common outcome measures in clinical examination on melasma. Since it is with no invasive nature, current studies applied the MASI or mMASI scores before and after the treatments to evaluate the effectiveness of the treatments [10]. On the other hand, MASI or mMASI is a relative and complex score, which is

This work is licensed under a Creative Commons Attribution 4.0 License. For more information, see https://creativecommons.org/licenses/by/4.0/

dependent on the dermatologists' experience and naked eye to evaluate, with no histopathological information. A quantitative non-invasive clinical microscopy to be able to provide both absolute melanin quantity and histopathological cellular morphometrics, especially melanocyte dendricity, in melasma patients for dermatologists to diagnose the pathological severity of melasma and to evaluate the effectiveness of treatments, may fulfill this clinical need.

There are a few in vivo optical technologies available to quantify melanin contents or to retrieve microscopy images inside human skin [11]–[15]; however, most of them still have some drawbacks. Diffuse reflectance spectroscopy (DRS) can quantify the absolute melanin quantity of human skin, but it lacks the information of depth and imaging capability [11]. Reflectance confocal microscopy (RCM) [12] and two-photon excitation microscopy (TPEM) [13] are both in vivo non-invasive imaging techniques that can only acquire relative rather than absolute melanin quantity. Recently, an in vivo label-free study reported that 1260 nm-based third harmonic generation (THG) microscopy can reveal strong THG contrasts with high specificity to dendritic melanocytes owing to the resonance THG enhancement due to the presence of melanin in focus [14]. With the same mechanism, absolute quantities of melanin of keratinocytes in human skin can be noninvasively measured by using third harmonic generation enhancement-ratio microscopy [15]. Combining THG with second harmonic generation (SHG) microscopy, Liao *et al.* pointed out that some structural variables, including the thickness of dermal papilla zone (DPZ) [16], [17] and the size of keratinocytes [17], [18], have a statistically significant relationship with intrinsic skin aging. Similarly, Kapsokalyvas *et al.* used in vivo SHG microscopy to measure and characterize the dermal papilla length, corresponding to DPZ thickness, in psoriatic and healthy skin as well [19].

In this study, we applied the in vivo slide-free label-free harmonic generation microscopy (HGM) to retrieve critical histopathological parameters for treatment assessment of melasma. These in vivo quantitative parameters include absolute melanin mass density (MMD) for keratinocytes in rete ridges, the melanocyte dendricity score (MDS) for dendritic melanin-producing melanocytes, the melanophage density (MPD) for irregular-shaped melanin-engulfing macrophages, and the thickness of dermal papilla zone (DPZ). Our clinical study indicated that these parameters were able to serve as clinical indices to evaluate the histopathological characteristics of melasma patients and the effectiveness of treatments. With 33 Asian female melasma patients, this HGM study showed that MMD, MDS, and MPD in melasma lesions were significantly higher than those in the surrounding normal skin; while DPZ in melasma lesions was significantly lower than the surrounding normal. After treatment, the MMD, MPD, and DPZ were found to be restored toward the normal level; however, we observed no significant MDS change. As a result, our study further supports the capability of 1260 nm-based HGM for the treatment assessment of melasma with quantitative histopathological parameters.

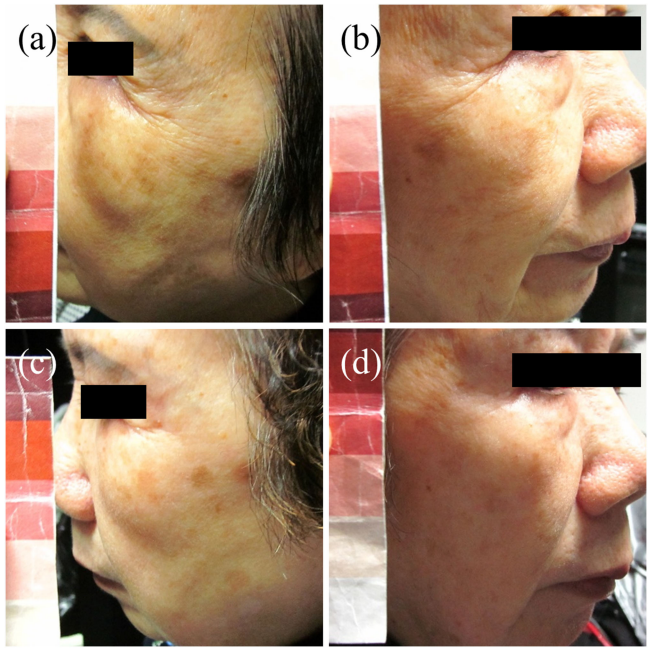

Fig. 1. (a) and (b) are the left face and right face of a melasma patient, respectively, before treatment (week 0). (c) and (d) are the left face and right face of a melasma patient, respectively, after treatment (week 12).

II. Methods

A. Study Population and Clinical Trials

In this research, 33 Asian women, between 37 to 72 years old and having symmetrically distributed melasma on the cheeks, of Fitzpatrick skin phototypes III to IV were recruited. We excluded subjects suffering from infection or wounds on the face.

This is a split-face, randomized and controlled study comparing the use of topical triple combination bleaching agent along (left side, TTT group) and the combination of low-fluence Q-switched (QS) neodymium-doped yttrium aluminum garnet (Nd:YAG) laser with the topical treatment (right side, TTT+QSNYL group) in melasma patients. All facial lesions were treated once at night for 12 weeks with a topical triple-combination agent mixing hydroquinone cream 4%, tretinoin cream 0.05%, and fluticasone propionate cream 0.05% in a 1:1:1 ratio. At weeks 5 and 7, low-fluence (1064 nm, 6 mm spot size, 2.5-3.0 J/cm^2, 10 Hz) QS Nd:YAG laser (MedLite C6, Hoya ConBio, Fremont, CA) illumination was performed on the right side with the endpoint of mild erythema.

Modified MASI (mMASI) was calculated for each side of the face as follows: mMASI = Area (A) $*$ [Darkness (D) + Homogeneity (H)] – before and 12 weeks after the treatment process [Fig. 1]. The calculation is based on the percentage of involved area (A = 0–6: 0 = 0%, 1 = 10%, 2 = 10–29%, 3 = 30–49%, 4 = 50–69%, 5 = 70–89%, 6 = 90–100%); darkness of pigment (D = 0–4: 0 = absent or normal skin color without evidence of hyperpigmentation, 1 = slight visible hyperpigmentation, 2 = mild visible, 3 = marked, 4 = severe), and homogeneity or density of hyperpigmentation (number of

pigmented lesions per unit facial area; H = 0–4: 0 = minimal, 1 = slight, 2 = mild, 3 = marked, 4 = severe). Thirty-one volunteers finished the whole two-acquisition process, while the other two came for their pre-treatment acquisition only. For an extensive discussion on the possible photodamage, please refer to Ref. [20]. Same as Ref. [20], no optical damage during the HGM image acquisition was observed as evaluated by the dermatologists (YHL, YSS). The total HGM image acquisition time for each visit is less than 30 minutes.

The entire protocol was approved by the Research Ethics Committee of National Taiwan University Hospital (NTUH-REC No.:201209069DOC), and informed consent was obtained from each subject prior to study entry. This study was conducted according to the Declaration of Helsinki Principles.

B. In Vivo HGM 3D Image Stacks of Human Skin

We acquired the SHG and THG signals using HGM with a 1260 nm femtosecond Cr:forsterite laser [14]–[18], [20]–[22]. The backward epi-SHG and epi-THG signals were collected to form an in vivo human skin *en face* image with a 295 × 295 μm field of view (FOV) at 15 frames per second (FPS), with 512 × 512 pixels. The 14-bit pseudo-color HGM 3D image stacks including 100 frames and 2 channels were obtained through the epidermis and the upper dermis with a total depth of 180 μm, and the transverse resolution was approximately 0.5 μm. For system details, please refer to Ref. [20]. Seriously saturated or blurred images were excluded. The in vivo 3D HGM image stacks consist of 2D images of different layers from the surface of epidermis to the upper dermis. Moving down into the skin, the stratum corneum (SC), stratum granulosum (SG), stratum spinosum (SS), stratum basale (SB), dermal papilla (DP), and reticular dermis (RD) appear in order [16], [17], [21], [22]. Fig. 2(a-f) shows different layers of epidermis and upper dermis of melasma patients. The HGM images contain THG and SHG signals, which are expressed in pseudo colors (magenta and green, respectively). The cells in the epidermis, such as keratinocytes, and the collagen fibers in the dermis can be identified via the pseudo colors.

The XZ or YZ transverse images can be derived by image reconstruction, and the rete ridges (RR) and the dermal papillae (DP) can also be shown in Fig. 2(g)(YZ-section).

In HGM images, well-trained dermatologists can identify the activated melanocytes by their dendrites in the lower epidermis and the melanophages in the upper dermis.

C. Thickness of Dermal Papilla Zone (DPZ)

The same definition of DPZ proposed by Liao *et al.* was used in the analyses [16], [17]. The upper boundary of DPZ was defined at the level where DP disappeared. The lower boundary of DPZ was defined at the level where SB disappeared. The stacked images of DPZ in human skin mostly consist of basal cells in SB (THG, shown in magenta) and collagen fibers in DP (SHG, shown in green).

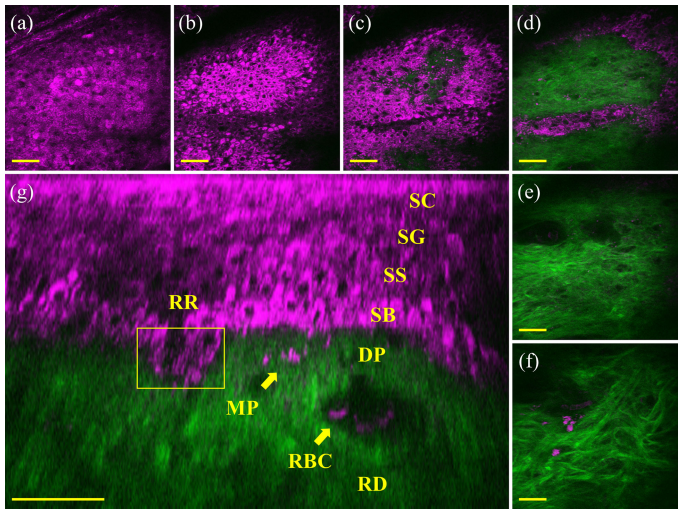

Fig. 2. (a)-(f) are the HGM acquired in vivo 2D images at depths of (a) 34.2, (b) 70.2, (c) 86.4, (d) 106.2, (e) 120.6, (f) 142.2 μm from the surface of melasma lesion on face. (a) and (b) show keratinocytes at different depths of the epidermis. (c) is the layer as the top of dermal papilla zone (DPZ), where the collagen fibers (shown in green SHG signals) start to appear. (d) is a typical image in the DPZ and shows both basal cells and collagen fibers. (e) is the layer at the bottom of DPZ, where the basal cells (shown in magenta THG signals) disappear. In this case, the thickness of DPZ is 120.6-86.4 = 34.2 μm. (e) and (f) are typical in vivo HGM images in the dermis and show collagen fibers at different depths of the dermis. In (g), the YZ-transverse-section image is derived from the same 3D image stack by image reconstruction. This sectional image of human skin shows several different layers, including the stratum corneum (SC), stratum granulosum (SG), stratum spinosum (SS), stratum basale (SB), dermal papilla (DP), and the upper reticular dermis (RD). The rete ridge (RR) is the downward projection of the epidermis between the dermal papillae. In this case, the macrophages (MP) and the trace of red blood cells (RBC) can also be found in the dermis of this HGM image. Scale bar = 50 μm. THG and SHG are shown in magenta and green pseudo color, respectively.

D. Melanocyte Dendricity score (MDS)

Besides basal keratinocytes, the basal layer in the epidermis contains melanocytes. The melanin-containing melanocytes have dendrites to transport melanosomes. The dendrite length can be significantly increased especially when melanocytes are hyperactive. In human skin HGM images, the well-trained dermatologists can distinguish the active melanocytes near the basal layers by melanocyte dendrites [14], and then evaluate the "dendritic ratio" (area with dendritic cells / area with cells) to determine the melanocyte dendricity score (MDS) from the THG images of the two layers above the upmost SHG-signal-containing layer (dermo-epidermal junction) in an HGM 3D image stack. The melanocyte dendricity score (MDS) is reported on a 4-point scale as follows: 3 is given for high dendritic ratio (70% and above), 2 for medium (30%-70%), 1 for low (<30%, except 0) and, 0 for no dendritic cells (0%) [Fig. 3].

E. Melanophage Density (MPD)

The melanophages are melanin-containing macrophages, the macrophages which have phagocytosed melanin, and they are frequently found in pigmented skin lesions. The melanophage density in the upper dermis is the average number

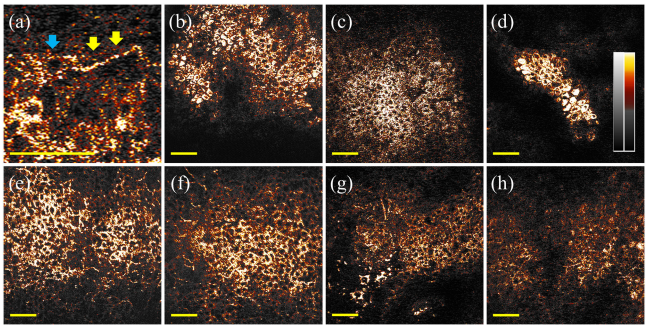

Fig. 3. Representative in vivo THG human skin images with different melanocyte dendricity scores (MDS). To enhance the contrast, the 14-bit pseudo-color THG images of melanocytes were converted from 14-bit grayscale THG images via a Look-Up Table (LUT) named "Smart", using the built-in function of ImageJ software (ver.1.50i, NIH, USA). (a) A typical melanocyte in the THG human skin image with a cell body (blue arrow) and an obvious long dendrite (yellow arrow). (b)(c)(d) Examples of THG human skin images with the lowest MDS equivalent to 0. (e)(f)(g)(h) Examples of THG human skin images with the highest MDS equivalent to 3. Scale bar = 50 μm.

of melanophages per square millimeter in the basal layer counted by dermatologists from the HGM image with the pre-processing for color-coding [Fig. 4].

F. Melanin Mass Density (MMD) of Keratinocytes in Rete Ridges

Following the method reported in Ref. [15], [23], the MMD of the keratinocytes in rete ridges can be acquired from every frame with both clear keratinocytes in rete ridges and collagen fibers in DPZ. We analyzed four frames in DPZ of a single HGM image stack and then got the average MMD of a stack. We analyzed one to three clearer stacks (depend on the image quality) in melasma lesion group and one clearest stack in normal group. Then the MMD of the keratinocytes in rete ridges in both the melasma lesions and surrounding normal skin can be quantified.

Because the HGM images sometimes contained parts of saturated pixels in THG signals, we adopted a protocol to calibrate the average THG intensity of a single frame. We got the histogram of the intensity from one THG frame with an ROI cell mask and then removed all the pixels with intensity equal to 16383, the saturated threshold for 14-bit images. A fitted normal distribution with a mean and a standard deviation could be acquired from our MATLAB code containing a built-in fitting function in MATLAB. Then all the removed pixels were redistributed to the part over the saturated threshold of the histogram in proportion by the fitted normal distribution curve. Then the calibrated average $\mathrm{THG}_{\mathrm{cytoplasm}}$ in the saturated images could be acquired from the histogram of THG intensity to replace the original number for analysis in this study.

G. Statistical Analysis

All the statistical results were all expressed as mean $\pm$ standard deviation (SD). The two-tailed paired *t*-tests were performed with the Microsoft Excel 2016 and OriginPro 2018 software, and $P < 0.05$ was considered statistically significant. (NS, no significance. $*$, $P < 0.05$. $**$, $P < 0.01$. $***$, $P < 0.001$.)

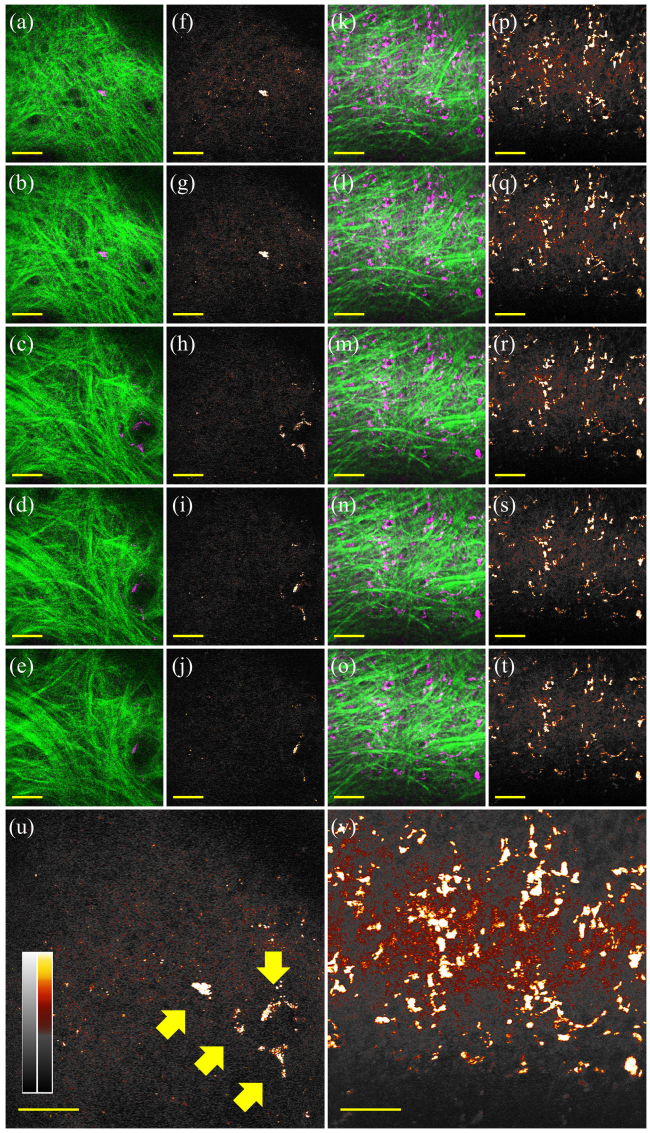

Fig. 4. Representative in vivo THG and HGM human skin images with different melanophage densities (MPD). (a)-(e) A serial HGM unstacked images in the dermis. (f)-(j) The color-coded THG images correspond to (a)-(e). (k)-(o) A serial HGM unstacked images in the dermis with higher MPD. (p)-(t) The color-coded THG images correspond to (k)-(o). Color coding follows the same table as Fig. 3. (u) The stacked THG image of (f)-(j). There are 4 melanophages (yellow arrows) in this stacked THG image (MPD = 44.4 cells/mm^2). (v) The stacked THG image of (p)-(t). There are 44 melanophages in this stacked THG image (MPD = 488.9 cells/mm^2). Scale bar = 50 μm; Z step = 1.8 µm.

At least three image stacks in the lesion and one image stack in the surrounding normal skin were acquired on either side of the face. For one subject, the results on all available images were averaged before the statistical analysis.

III. Results and Discussion

A. mMASI and Darkness of mMASI

After subject recruitment, the conventional visual mMASI score and its several subcomponents, including the darkness (D), were acquired to evaluate the weighted pathologies of each

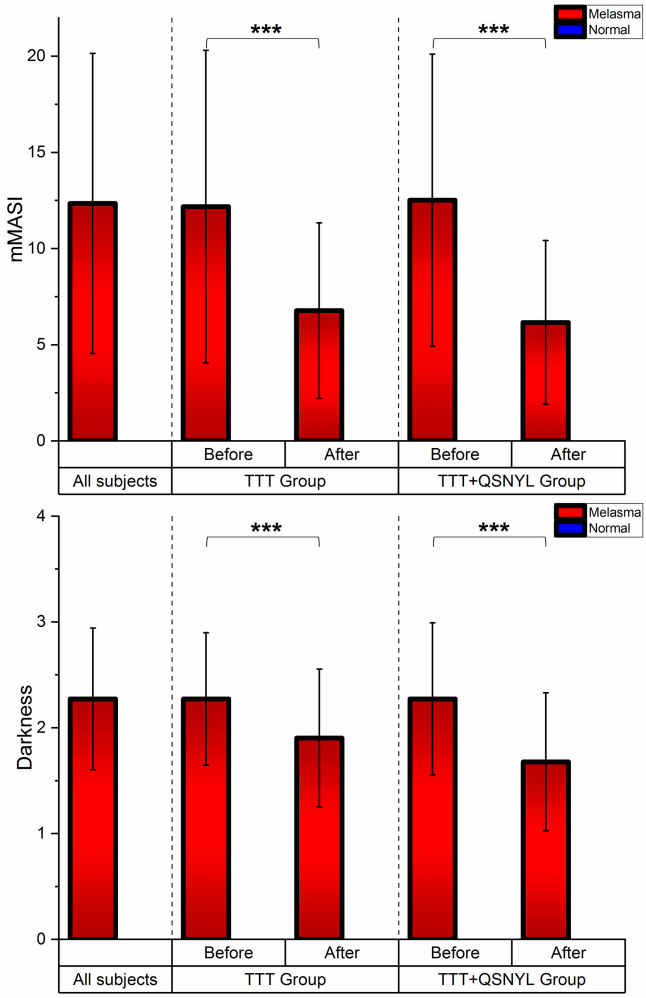

Fig. 5. The results of the mMASI and the average darkness (D) subcomponent in all the subjects including the TTT and the TTT+QSNYL groups. The TTT group was the subjects having their left face treated with topical cream. The TTT+QSNYL group was the subjects having their right face treated with the combination therapy containing both the topical and laser treatments. The average mMASI (TTT: 12.2 and 6.8 respectively, $P = 0.0006$; TTT+QSNYL: 12.5 and 6.2 respectively, $P = 0.0001$), as well as the average darkness (D) subcomponent (TTT: 2.3 and 1.9 respectively, $P = 0.0006$; TTT+QSNYL: 2.3 and 1.7 respectively, $P = 0.0001$), in the melasma lesions decreased significantly after treatment. $***$, $P < 0.001$.

melasma patient before and after treatment. Both mMASI and D significantly decreased after treatments [Fig. 5].

B. Thickness of Dermal Papilla Zone (DPZ)

In previous research, skin aging has been demonstrated to be associated with flattening of the dermal-epidermal junction, so the thickness of DPZ is expected to decrease with age [16], [17]. Likewise the dermal papilla length, corresponding to DPZ thickness, in psoriatic and healthy skin are significantly different [19]. Thus, the thickness of DPZ may also be a meaningful parameter as an index for some skin disorders [19] such as melasma. The results show that the DPZ of the melasma lesions is significantly thinner than the surrounding normal skin. The average DPZ in all subjects is 18.3 and 32.6 μm in melasma

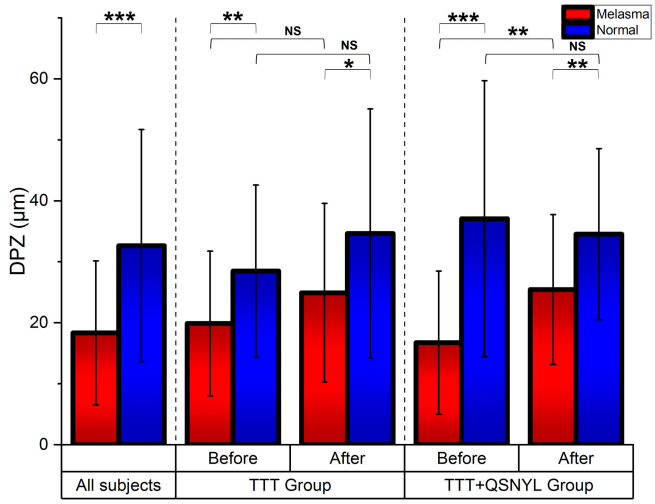

Fig. 6. The results of the DPZ in all the subjects, the TTT and TTT+QSNYL groups. The average DPZ of melasma lesions is significantly lower than the surrounding normal skin (All subjects: 18.3 and 32.6 μm in melasma and normal skin respectively, $P = 0.0000009$; TTT: 19.9 and 28.5 μm respectively, $P = 0.0045$; TTT+QSNYL: 16.7 and 37.1 μm respectively, $P = 0.00004$). The average DPZ in the melasma lesions increased significantly after combination therapy but only increased slightly with no significant difference after topical treatment (TTT: 19.9 and 24.9 μm respectively, $P = 0.3047$; TTT+QSNYL: 16.7 and 25.5 μm respectively, $P = 0.0058$). The baseline DPZ in the surrounding normal skin didn't change significantly after treatments (TTT: 28.5 and 34.6 μm respectively, $P = 0.0564$; TTT+QSNYL: 37.1 and 34.5 μm respectively, $P = 0.7017$). NS, no significance. $*$, $P < 0.05$. $**$, $P < 0.01$. $***$, $P < 0.001$.

and normal skin respectively ($P = 0.0000009$), in the TTT group is 19.9 and 28.5 μm respectively ($P = 0.0045$), and in TTT+QSNYL group is 16.7 and 37.1 μm respectively ($P = 0.00004$) [Fig. 6]. This result implies that the DPZ parameter can be an effective index to evaluate the severity of melasma besides the mMASI score.

As a result, we found DPZ could also be acquired to evaluate the effectiveness of treatments. In this study, combination treatment with topical cream and laser could partially recover the thickness of DPZ in melasma lesion after treatment (TTT+QSNYL group: 16.7 and 25.5 μm, before and after treatment respectively: $P = 0.0058$) [Fig. 6]; on the contrary, treatment with only topical cream did not (TTT group: 19.9 and 24.9 μm, before and after treatment respectively; $P = 0.3047$) [Fig. 6]. With partially recovered DPZ thickness, the melanin in the dermis layer will be further away from the surface for visualization.

These results related to the DPZ parameter point out the potential similarity in the reduction of DPZ caused by melasma and skin aging. The finding of decreased DPZ could be regarded as a common pathological phenomenon of melasma and skin aging; fortunately, such decreased DPZ caused by melasma could be recovered by combination treatment with topical cream and low-fluence QS Nd: YAG laser. Therefore, melasma could be considered as a local and partially recoverable "equivalent skin photoaging".

Through DPZ thickness, we observed a different effect of the two treatments used in this study. In terms of DPZ recovery, the combination therapy with topical cream and laser is more effective than topical treatment along. Unlike the topical treatment,

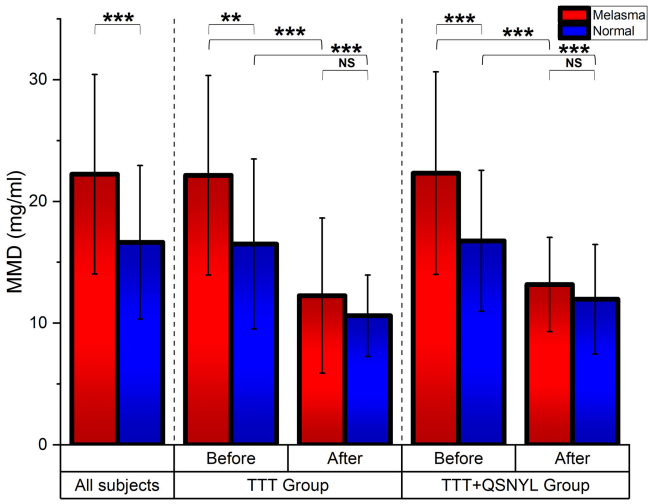

Fig. 7. The results of the MMD in all the subjects, the TTT and TTT+QSNYL groups. The average MMD of the keratinocytes in the rete ridge of melasma lesions is significantly higher than the surrounding normal skin (All subjects: 22.2 and 16.6 mg/ml respectively, $P = 0.0000037$; TTT: 22.1 and 16.5 mg/ml respectively, $P = 0.0049$; TTT+QSNYL: 22.3 and 16.8 mg/ml respectively, $P = 0.0003$). The average MMD in the melasma lesions decreased significantly after treatments (TTT: 22.1 and 12.3 mg/ml respectively, $P = 0.0004$; TTT+QSNYL: 22.3 and 13.2 mg/ml respectively, $P = 0.0003$). The average MMD in the surrounding normal skin decreased significantly after treatments (TTT: 16.5 and 10.6 mg/ml respectively, $P = 0.0006$; TTT+QSNYL: 16.8 and 12.0 mg/ml respectively, $P = 0.0002$). NS, no significance. $**$, $P < 0.01$. $***$, $P < 0.001$.

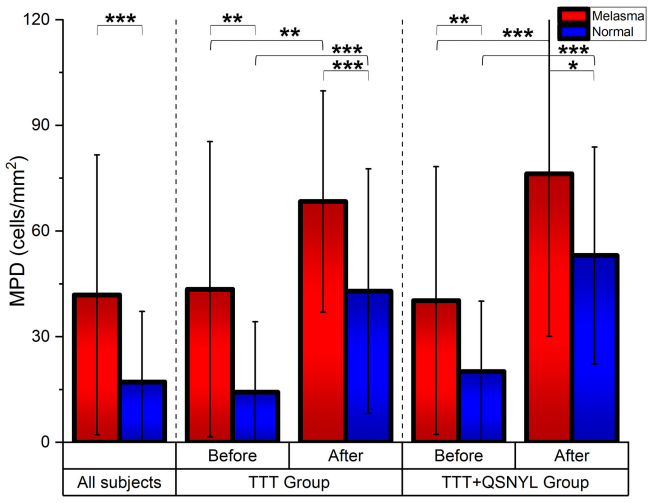

Fig. 8. The results of the MPD in all the subjects, the TTT and TTT+QSNYL groups. The average MPD of the melasma lesions is significantly higher than the surrounding normal skin (All: 41.9 and 17.1 cells/mm^2 respectively, $P = 0.00001$; TTT: 43.5 and 14.3 cells/mm^2 respectively, $P = 0.0016$; TTT+QSNYL: 40.3 and 20.1 cells/mm^2 respectively, $P = 0.0023$). The average MPD in the melasma lesions increased significantly after treatments (TTT: 43.5 and 68.4 cells/mm^2 respectively, $P = 0.0049$; TTT+QSNYL: 40.3 and 76.3 cells/mm^2 respectively, $P = 0.0004$). The average MPD in the surrounding normal skin increased significantly after treatments (TTT: 14.3 and 42.9 cells/mm^2 respectively, $P = 0.000001$; TTT+QSNYL: 20.1 and 53.1 cells/mm^2 respectively, P = 0.000001). $*$, $P < 0.05$. $**$, $P < 0.01$. $***$, $P < 0.001$.

which did not significantly recover the decreased DPZ caused by melasma, the combination therapy significantly recovered the thickness of DPZ. Even though the decreased DPZ reverted toward the normal level, yet the restored DPZ thickness was still significantly lower than the surrounding normal skin. As for the topical cream containing hydroquinone, tretinoin, and fluticasone propionate, it may not significantly affect the structure of dermal-epidermal junction (DEJ). In contrast, low-fluence 1064-nm QS Nd:YAG laser treatment in the combination therapy could penetrate into the dermis and impact pigment-containing cells in the basal layer and upper dermis. Therefore, remodeling of dermal-epidermal junction could be possibly contributed by the add-on 1064-nm QS Nd:YAG laser treatment [24].

C. Melanin Mass Density (MMD)

The average MMD of the keratinocytes in the rete ridges of melasma lesions is significantly higher than the surrounding normal skin (All subjects: 22.2 and 16.6 mg/ml respectively, $P = 0.0000037$) [Fig. 7]. This result is consistent with the diagnosis of the dermatologist, which implies that the MMD parameter can be an effective index to evaluate the pathological severity of melasma besides the mMASI score.

In this study, the average MMD in the melasma lesions decreased significantly after the topical cream treatment as well as the combination therapy (TTT: 22.1 and 12.3 mg/ml respectively, $P = 0.0004$; TTT+QSNYL: 22.3 and 13.2 mg/ml respectively, $P = 0.0003$), as summarized in Fig. 7.

It is interesting to notice that after treatments, the average MMD in the surrounding normal skin also decreased significantly due to the application of the topical cream. More importantly, after treatment, there are no significant differences between the average MMD in the melasma lesions and the surrounding normal skin. This shows that both treatments can decrease the differences of the pigments between the melasma lesions and adjacent areas, which is the main focus of the therapy.

D. Melanophage Density (MPD)

The average MPD of the melasma lesions was found to be significantly higher than the surrounding normal skin (All: 41.9 and 17.1 cells/mm^2 respectively, $P = 0.00001$ [Fig. 8]. Furthermore, the average MPD in the melasma lesions increased significantly after treatments (TTT: 43.5 and 68.4 cells/mm^2 respectively, $P = 0.0049$; TTT+QSNYL: 40.3 and 76.3 cells/mm^2 respectively, $P = 0.0004$). The average MPD in the surrounding normal skin also increased after treatments (TTT: 14.3 and 42.9 cells/mm^2 respectively, $P = 0.000001$; TTT+QSNYL: 20.1 and 53.1 cells/mm^2 respectively, $P = 0.000001$) [Fig. 8].

Before treatment, the average MPD of the melasma lesions is significantly higher than the surrounding normal skin due to severer pigmentation, in consistent with the mMASI score. After treatment, the increase of the average MPD either in the melasma lesions or the normal adjacent area can be attributed to the treatment effect. The melanophages in the dermis of human skin are the phagocytes that engulf the redundant melanin. We attribute the increase of MPD to the treatments' result of

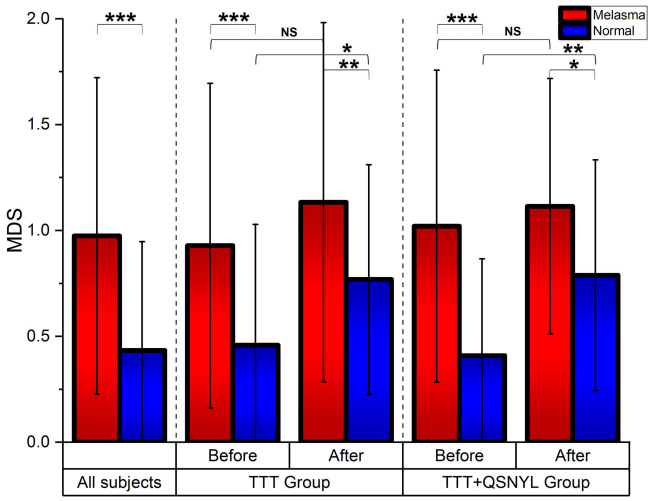

Fig. 9. The results of the MDS in all the subjects, the TTT groups, and the TTT+QSNYL groups. The TTT groups are the results of left face with the topical cream treatment. The TTT+QSNYL groups are the results of right face with the combination therapy containing both the topical cream treatment and laser treatment. The average MDS of the melasma lesions is significantly higher than the surrounding normal skin (All: 0.97 and 0.43 respectively, $P = 0.00000000019$; TTT: 0.93 and 0.46 respectively, $P = 0.0003$; TTT+QSNYL: 1.02 and 0.41 respectively, $P = 0.0000001$). The average MDS in the melasma lesions did not increase significantly in spite of the slight rise of the mean value after treatments (TTT: 0.93 and 1.13 respectively, $P = 0.2608$; TTT+QSNYL: 1.02 and 1.11 respectively, $P = 0.3800$). The average MDS in the surrounding normal skin increased significantly after treatments (TTT: 0.46 and 0.77 respectively, $P = 0.0208$; TTT+QSNYL: 0.41 and 0.79 respectively, $P = 0.0091$). NS, no significance. $*$, $P < 0.05$. $**$, $P < 0.01$. $***$, $P < 0.001$.

dropping down the photodamaged melanin fragment from the epidermis to the dermis layer.

E. Melanocyte Dendricity Score (MDS)

Since melasma is caused by hyperactivation of melanocytes, a noninvasive way to evaluate the melanocyte's hyperactivation, the keystone of melasma's mechanism, is critical.

The analysis results show that the average MDS of the melasma lesions is significantly higher than the surrounding normal skin (All subjects: 0.97 and 0.43 respectively, $P = 0.00000000019$) [Fig. 9]. This result implies that the MDS parameter could be an effective index to evaluate the pathological severity of melasma besides the mMASI score and conventional biopsy for dermatologists. On the other hand, the average MDS in the melasma lesions did not decrease significantly after treatment. Instead, the minor rise of the mean value can be found after treatments (TTT: 0.93 and 1.13 respectively, $P = 0.2608$; TTT+QSNYL: 1.02 and 1.11 respectively, $P = 0.3800$). Even worse, the average MDS in the surrounding normal skin increased significantly after treatments (TTT: 0.46 and 0.77 respectively, $P = 0.0208$; TTT+QSNYL: 0.41 and 0.79 respectively, $P = 0.0091$), indicating the activation of the melanocytes due to treatment stimulation.

Previous studies [3], [6]–[8] show that the hyperactivity of melanocytes has a strong positive correlation with the pathological severity of melasma. The unexpected results after treatments suggested that some treatments might remove the melanin in the epidermal keratinocytes but stimulate the melanocyte activity so that the density of melanocytic dendrites increase. Even though more studies, especially longitudinal studies, should be performed, our observation might be related to the relapse of the skin disorder after treatment.

F. Melanocyte-Hyperactivation Case Ratio

It is worth noting that before treatment the MDS, MMD, and MPD parameters of the melasma lesions were all significantly higher than the surrounding normal skin. The observed increase of MDS is consistent with our understanding regarding the melasma's possible pathogenesis, while the observed MMD increase is the result of the melanocyte hyperactivation. With the overproduction of melanin, the melanophages gathered to engulf the excessive melanin, leading to the increased MPD.

After treatments, these three parameters responded in different ways. Treatments removed the excess melanin, leading to the decreased MMD. To remove the dropped down melanin, phagocytes were attracted and gathered to engulf those excess melanin, leading to the increased MPD. As for the MDS in the melasma region, which could be the most essential score, we observed no significant increase nor decrease in the score statistically.

To further investigate the potential role of hyperactivation of melanocytes, we studied the population of melasma patients with a higher MDS. We defined the melanocyte-hyperactivation case ratio as the population ratio of the melanocyte-hyperactivation cases, whose melanocyte activity or number analyzed from the histopathological images in melasma group is higher than that in normal skin. As a result, in this research, the case ratio provided by THG microscopy is 29 (cases with a higher MDS in melasma group than that in normal skin) out of 33 (all cases), equivalent to 88%. Under the same definition, the melanocyte-hyperactivation case ratio calculated from the ex vivo study by using conventional biopsy with suitable immunostaining for melanocytes is 47 out of 56 cases, equivalent to 84% [7]. This agreement supports not only the primary role of melanocyte hyperactivation in melasma, but also the high specificity of HGM to melanocyte dendrites. In contrast, the melanocyte-hyperactivation case ratio calculated from several in vivo studies by using RCM to image the dendritic-shaped cells were all less than 25% (12.5%, 20.0%, 23.1%) [25]–[27]. We attribute the difference between our HGM results and previous RCM results to the lower specificity of RCM to melanocyte dendrites. In a previous RCM study [28], the dendritic cells in the spinous layer, found in 5/15 cases (33.3%), were interpreted as activated Langerhans cells more than melanocytes. Several studies [14], [29]–[31] indicate that current RCM system is hard to differentiate dendritic Langerhans cells from dendritic melanocytes. On the other hand, by using conventional ex vivo biopsy with suitable immunostaining, for example, HMB-45 [14], [30] and CD-1a [7], [14], [27], [29]–[31], researchers can specifically identify melanocytes and Langerhans cells respectively.

Compared with the lower case ratio ($<25\%$) given by RCM, the ratio (88%) given by melanocyte-dendricity-sensitive THG microscopy is close to the ratio (84%) given by biopsy with

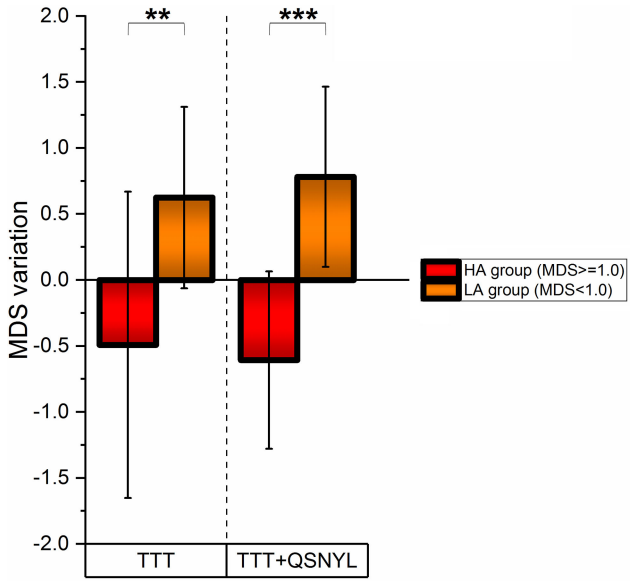

Fig. 10. The advanced analysis results of the MDS variation in the TTT group and TTT+QSNYL group. The average MDS variation in the TTT and TTT+QSNYL groups between HA and LA group (MDS $>=$ 1.0 and MDS $<$ 1.0, respectively) are significantly different. In other words, the in vivo melanocyte activity in melasma lesion in HA group decreased after treatment; on the contrary, that in LA group increased. $**$, $P < 0.01$. $***$, $P < 0.001$.

suitable immunostaining for melanocytes, supporting the high specificity of the adopted THG microscopy to melanocyte-dendricity and its capability to differentiate melanocyte-dendricity from dendritic Langerhans cells. This closer ratio once again supports that the THG-based melanocyte dendricity score can suitably reflect melanocyte dendricity of melasma.

To further pursue the treatment responses with different MDS, we divided the subjects into high (HA) and low (LA) activation groups based on high (MDS$>=1.0$) and low (MDS<1.0) MDS values, respectively. Further analysis [Fig. 10] showed that the in vivo melanocyte activity in melasma lesion in HA group decreased after treatment; on the contrary, that in LA group increased. The different melanocyte activity between these two groups before treatment caused different treatment outcomes, indicating the importance of pretreatment MDS score, which would eventually result in different treatment decisions in the future.

G. Potential for Quantitative Assessment of Melasma

According to the above results, the histopathological parameters MDS, MMD, MPD, and DPZ provided by HGM can be considered as metrics or biomarkers for quantitative assessment of melasma – as well as other similar pigmentary skin disorders – and its treatment.

The DPZ can reflect structural changes in human skin, potentially implying changes in elasticity, and correspond to equivalent skin photoaging. Clinicians can assess the degree of recovery for patients with DPZ thickness after various treatments. Besides DPZ, three melanin-related parameters MDS, MMD, and MPD can potentially assess the synthesis, density, and the amount of on-going melanin removal.

Compared with the relative, weighted, and subjective mMASI score as well as its subcomponent the darkness (D), MMD and MPD can reflect histopathological characteristics and pathologies and act as absolute, particular, objective indices; moreover, the two indices may potentially demonstrate the melanin content at each specific depth and even the vertical distribution of melanin. Based on the vertical distribution of melanin, MMD and MPD can represent the amount of epidermal and dermal melanin content, which may help clinicians differentiating epidermal and mixed (epidermal and dermal) types of melasma [5].

Admittedly, MMD and MPD can reflect just the physiological phenomenon rather than the disease activity; in contrast, MDS can reflect the disease activity of melasma and hence may potentially assess the histopathological severity of melasma. Besides being helpful in diagnosis, MDS can non-invasively assess different melasma treatments and help dermatologists make treatment decisions. For instance, in this study, MDS can provide advanced suggestions to clinicians that melasma lesions with higher MDS (HA group) can more likely get beneficial therapeutic effects in decreasing melanocyte activity; while those with lower MDS (LA group) may not. Besides the lesions with lower MDS, the surrounding normal skin, also with lower MDS but without apparent clinical abnormality, is recommended not to be treated. In this case, the topical cream is suggested to apply only on lesions with higher MDS instead of on all the face.

Altogether, MDS provides quantitative information to show the activity of melasma, not only for predicting the therapeutic effects but also for predicting the relapse of melasma. Clinicians might no longer be confused by the various responses of melasma patients.

IV. Conclusion

In conclusion, HGM is capable of providing both the in vivo non-invasive human skin images and the cellular morphometrics of melanin-containing cells from the skin of melasma patients. As the diagnosis and treatment indices of melasma for the dermatologists, the cellular morphometrics provided by HGM include the absolute melanin mass density (MMD), the melanocyte dendricity score (MDS), the melanophage density (MPD), and the thickness of dermal papilla zone (DPZ). Different from the traditional invasive biopsy, treatment assessment becomes possible since the lesions were removed after biopsy so that longitudinal studies on the same location were impossible. HGM can thus serve as a suitable label-free slide-free trauma-free imaging tool with cellular details for treatment assessment, complementary to the subjective mMASI scores. In this study, we applied HGM for the treatment assessment of a split-face study of melasma with triple topical bleaching agent along and the combination of low-fluence QS Nd:YAG laser with the topical treatment. Before treatment, the MDS, MMD, and MPD parameters of the melasma lesions were all significantly higher than the surrounding normal skin, while the DPZ parameter was

significantly lower. The observed increase of MDS is consistent with our understanding regarding the melasma's possible pathogenesis: melanocyte hyperactivation, while the observed MMD increase is the result of it. With the overproduction of melanin, the melanophages gathered to engulf the excessive melanin, leading to the increased MPD.

After treatment, the MDS, MMD, and MPD parameters responded in different ways. Treatments removed the excess melanin, leading to the decreased MMD. To remove the dropped down melanin, phagocytes were attracted and gathered to engulf those excess melanin fragments, leading to the increased MPD. As for the MDS in the melasma region, we observed no significant increase nor decrease in the score statistically. For the tissue level DPZ, moderate recovery toward the normal level was observed. Our study supports not only the capability of HGM for quantitative treatment assessment of melasma, but also the high specificity of HGM to the dendricity of melanocytes, which is a critical diagnosis parameter of melasma.

Acknowledgment

The authors would like to thank for the prototype of the MATLAB code by Prof. Gwo-Giun Chris Lee's Lab and the modification of the MATLAB code by Yu-Hsiang Su and Kuan-Hung Lin. M.-L. Wei would like to thank for the help of clinical trials by Guan-Liang Lin and the English writing by Jie-Wei Jiang and Derek Yang.

References

[1] A. Sivayathorn, "Melasma in orientals," *Clin. Drug Investigation,* vol. 10, no. 2, pp. 34–40, 1995.
[2] P. L. Chandravathi, D. Soujanya, and H. Karani, "Clinico epidemiological and biochemical profile of patients with melasma," *J. Evol. Med. Dent. Sci.,* vol. 4, no. 81, pp. 14115–14124, 2015.
[3] W. Kang *et al.*, "Melasma: Histopathological characteristics in 56 korean patients," *Brit. J. Dermatol.,* vol. 146, no. 2, pp. 228–237, 2002.
[4] S.-H. Kwon, Y.-J. Hwang, S.-K. Lee, and K.-C. Park, "Heterogeneous pathology of melasma and its clinical implications," *Int. J. Mol. Sci.,* vol. 17, no. 6, pp. 824, 2016.
[5] O. A. Ogbechie-Godec and N. Elbuluk, "Melasma: An up-to-date comprehensive review," *Dermatol. Ther.,* vol. 7, no. 3, pp. 305–318, 2017.
[6] A. L. Akabane, I. P. Almeida, and J. C. L. Simão, "Analysis of melasma quality of life sca-les (MELASQoL and DLQI) and MASI in polypodium leucotomos treated patients," *Surg. Cosmetic Dermatol.,* vol. 37, no. 6.78, pp. 214.
[7] W. Kang *et al.*, "Melasma: Histopathological characteristics in 56 korean patients," *Brit. J. Dermatol.,* vol. 146, no. 2, pp. 228–237, 2002.
[8] H. Y. Kang *et al.*, "In vivo reflectance confocal microscopy detects pigmentary changes in melasma at a cellular level resolution," *Exp. Dermatol.,* vol. 19, no. 8, pp. e228–e233, 2010.
[9] A. G. Pandya *et al.*, "Reliability assessment and validation of the melasma area and severity index (MASI) and a new modified MASI scoring method," *J. Amer. Acad. Dermatol.,* vol. 64, no. 1, pp. 78–83. e2, 2011.
[10] S. H. Kong, H. S. Suh, and Y. S. Choi, "Treatment of melasma with pulsed-dye laser and 1,064-nm Q-switched nd: YAG laser: A split-face study," *Ann. Dermatol.,* vol. 30, no. 1, pp. 1–7, 2018.
[11] S.-Y. Tsui, C.-Y. Wang, T.-H. Huang, and K.-B. Sung, "Modelling spatially-resolved diffuse reflectance spectra of a multi-layered skin model by artificial neural networks trained with monte carlo simulations," *Biomed. Opt. Exp.,* vol. 9, no. 4, pp. 1531–1544, 2018.
[12] S. G. Lagarrigue *et al.*, "In vivo quantification of epidermis pigmentation and dermis papilla density with reflectance confocal microscopy: Variations with age and skin phototype," *Exp. Dermatol.,* vol. 21, no. 4, pp. 281–286, 2012.
[13] T. Baldeweck *et al.*, "3D Quantification of melanin in human skin in vivo based on multiphoton microscopy, image processing," in *Proc. Focus Micorscopy*,2013.
[14] W.-H. Weng *et al.*, "Differentiating intratumoral melanocytes from langerhans cells in nonmelanocytic pigmented skin tumors in vivo by label-free third-harmonic generation microscopy," *J. Biomed. Opt.,* vol. 21, no. 7, 2016, Art. no. 076009.
[15] C.-K. Sun *et al.*, "Slide-free clinical imaging of melanin with absolute quantities using label-free third-harmonic-generation enhancement-ratio microscopy," *Biomed. Opt. Exp.,* vol. 11, no. 6, pp. 3009–3024, 2020.
[16] Y.-H. Liao *et al.*, "Quantitative analysis of intrinsic skin aging in dermal papillae by in vivo harmonic generation microscopy," *Biomed. Opt. Exp.,* vol. 5, no. 9, pp. 3266–3279, 2014.
[17] K.-H. Lin, Y.-H. Liao, M.-L. Wei, and C.-K. Sun, "Comparative analysis of intrinsic skin aging between caucasian and asian subjects by slide-free in vivo harmonic generation microscopy," *J. Biophotonics,* vol. 13, no. 4, 2020, Art. no. e201960063.
[18] Y.-H. Liao *et al.*, "Determination of chronological aging parameters in epidermal keratinocytes by in vivo harmonic generation microscopy," *Biomed. Opt. Exp.,* vol. 4, no. 1, pp. 77–88, 2013.
[19] D. Kapsokalyvas *et al.*, "In-vivo imaging of psoriatic lesions with polarization multispectral dermoscopy and multiphoton microscopy," *Biomed. Opt. Exp.,* vol. 5, no. 7, pp. 2405–2419, 2014.
[20] Y.-H. Liao *et al.*, "In vivo third-harmonic generation microscopy study on vitiligo patients," *J. Biomed. Opt.,* vol. 25, no. 1, 2020, Art. no. 014504.
[21] S.-Y. Chen *et al.*, "In vivo virtual biopsy of human skin by using noninvasive higher harmonic generation microscopy," *IEEE J. Sel. Topics Quantum Electron.,* vol. 16, no. 3, pp. 478–492, May/Jun. 2010.
[22] M.-R. Tsai, C.-Y. Lin, Y.-H. Liao, and C.-K. Sun, "Applying tattoo dye as a third-harmonic generation contrast agent for in vivo optical virtual biopsy of human skin," *J. Biomed. Opt.,* vol. 18, no. 2, 2013, Art. no. 026012.
[23] C.-K. Sun, W.-M. Liu, and Y.-H. Liao, "Study on melanin enhanced third harmonic generation in a live cell model," *Biomed. Opt. Exp.,* vol. 10, no. 11, pp. 5716–5723, 2019.
[24] D. Goldberg and C. Metzler, "Skin resurfacing utilizing a low-fluence nd: YAG laser," *J. Cutan. Laser Ther.,* vol. 1, no. 1, pp. 23–27, 1999.
[25] C. Longo, G. Pellacani, A. Tourlaki, M. Galimberti, and P. L. Bencini, "Melasma and low-energy Q-switched laser: Treatment assessment by means of in vivo confocal microscopy," *Lasers Med. Sci.,* vol. 29, no. 3, pp. 1159–1163, 2014.
[26] K. Tsilika *et al.*, "A pilot study using reflectance confocal microscopy (RCM) in the assessment of a novel formulation for the treatment of melasma," *J. Drugs Dermatol,* vol. 10, no. 11, pp. 1260–1264, 2011.
[27] H. Y. Kang *et al.*, "In vivo reflectance confocal microscopy detects pigmentary changes in melasma at a cellular level resolution," *Exp. Dermatol.,* vol. 19, no. 8, pp. e228–e233, 2010.
[28] M. Ardigo, N. Cameli, E. Berardesca, and S. Gonzalez, "Characterization and evaluation of pigment distribution and response to therapy in melasma using in vivo reflectance confocal microscopy: A preliminary study," *J. Eur. Acad. Dermatol. Venereol.,* vol. 24, no. 11, pp. 1296–1303, 2010.
[29] A. L. C. Agero *et al.*, "Reflectance confocal microscopy of pigmented basal cell carcinoma," *J. Amer. Acad. Dermatol.,* vol. 54, no. 4, pp. 638–643, 2006.
[30] S. Segura, S. Puig, C. Carrera, J. Palou, and J. Malvehy, "Dendritic cells in pigmented basal cell carcinoma: A relevant finding by reflectance-mode confocal microscopy," *Arch. Dermatol.,* vol. 143, no. 7, pp. 883–886, 2007.
[31] P. Hashemi *et al.*, "Langerhans cells and melanocytes share similar morphologic features under in vivo reflectance confocal microscopy: A challenge for melanoma diagnosis," *J. Amer. Acad. Dermatol.,* vol. 66, no. 3, pp. 452–462, 2012.

Ming-Liang Wei received the B.S. and M.S. degrees from the National Taiwan University (NTU), Taipei, Taiwan. He is currently a Research Assistant with Molecular Imaging Center, NTU and works on studying the clinical application of HGM for skin pigmentation disorders and biomedical imaging analysis.

Yi-Hua Liao received the M.D. degree from the College of Medicine and the Ph.D. degree from the Graduate Institute of Pathology, College of Medicine, National Taiwan University, Taipei, Taiwan, in 1996 and 2007, respectively. She is currently an Associate Professor with the Department of Dermatology, National Taiwan University, and a Supervisor with Taiwanese Dermatological Association, Taipei. Her research interests include dermatologic surgery special clinic, cosmetic surgery, and laser special clinic.

Wei-Hung Weng received the M.D. degree from Chang Gung University, Taoyuan, Taiwan, in 2011 and M.M.Sc. degree in biomedical informatics from Harvard Medical School, Boston, MA, USA. He is currently working toward the Ph.D. degree with the Department of Electrical Engineering and Computer Science, Massachusetts Institute of Technology, Cambridge, MA, USA. His research interests include medical image analysis, and applying machine learning and natural language-processing methods to unstructured clinical data.

Yuan-Ta Shih received the Ph.D. degree from the Department of Biomedical Engineering, Chung-Yuan Christian University, Taoyuan City, Taiwan, in 2012. From 2012 to 2015, he was a Postdoctoral Fellow with the Molecular Imaging Center, National Taiwan University, Taipei, Taiwan. He is currently a Product Manager with Leadtek Research Inc., Taipei City, Taiwan, for developing biomedical signal analyzing algorithm and medical device. His main research interests include medical device development and biomedical signal analysis.

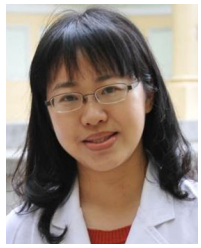

Yi-Shuan Sheen received the M.D. degree from the College of Medicine, Kaohsiung Medical University, Kaohsiung, Taiwan, in 2004 and the M.S. degree from the Graduate Institute of Clinical Medicine, National Taiwan University, Taipei, Taiwan, in 2009. She is currently an Assistant Professor with the Department of Dermatology, College of Medicine, National Taiwan University. Her research interests include melanoma, cutaneous carcinogenesis, and dermatologic surgery and lasers.

Chi-Kuang Sun (Fellow, IEEE) received the Ph.D. degree in applied physics from Harvard University, Cambridge, MA, USA, in 1995. From 1995 to 1996, he was an Assistant Researcher with the Center for Quantized Electronic Structures, University of California, Santa Barbara, Santa Barbara, CA, USA. In 1996, he joined National Taiwan University, where he is currently a Distinguished Professor of photonics and optoelectronics. He founded the Molecular Imaging Center, National Taiwan University, Taipei, Taiwan. His research interests include nano-acoustics, femtosecond optics, THz optoelectronics, and biomedical imaging. He is a fellow of the OSA and SPIE.